Journal Pre-proofs

Design, synthesis and biological evaluation of novel glyoxalase I inhibitors possessing diazenylbenzenesulfonamide moiety as potential anticancer agents

Buthina A. Al-Oudat, Hana'a M. Jaradat, Qosay A. Al-Balas, Nizar A. Al-Shar'i, Amanda Bryant-Friedrich, Mel F. Bedi

PII: S0968-0896(20)30438-7
DOI: https://doi.org/10.1016/j.bmc.2020.115608
Reference: BMC 115608

To appear in: *Bioorganic & Medicinal Chemistry*

Received Date: 19 March 2020
Revised Date: 19 June 2020
Accepted Date: 22 June 2020

Please cite this article as: Al-Oudat, B.A., Jaradat, H.M., Al-Balas, Q.A., Al-Shar'i, N.A., Bryant-Friedrich, A., Bedi, M.F., Design, synthesis and biological evaluation of novel glyoxalase I inhibitors possessing diazenylbenzenesulfonamide moiety as potential anticancer agents, *Bioorganic & Medicinal Chemistry* (2020), doi: https://doi.org/10.1016/j.bmc.2020.115608

Graphical Abstract

Design, synthesis and biological evaluation of novel glyoxalase I inhibitors possessing diazenylbenzenesulfonamide moiety as potential anticancer agents

Leave this area blank for abstract info.

Buthina A. Al-Oudat[a,*], Hana'a M. Jaradat[a], Qosay A. Al-Balas[a], Nizar A. Al-Shar'i[a], Amanda Bryant-Friedrich[b], Mel F. Bedi[b]

[a]*Department of Medicinal Chemistry and Pharmacognosy, Faculty of Pharmacy, Jordan University of Science and Technology, P.O. Box 3030, Irbid 22110, Jordan*
[b]*Department of Medicinal and Biological Chemistry, College of Pharmacy and Pharmaceutical Sciences, University of Toledo, Toledo, OH, 43606, USA*

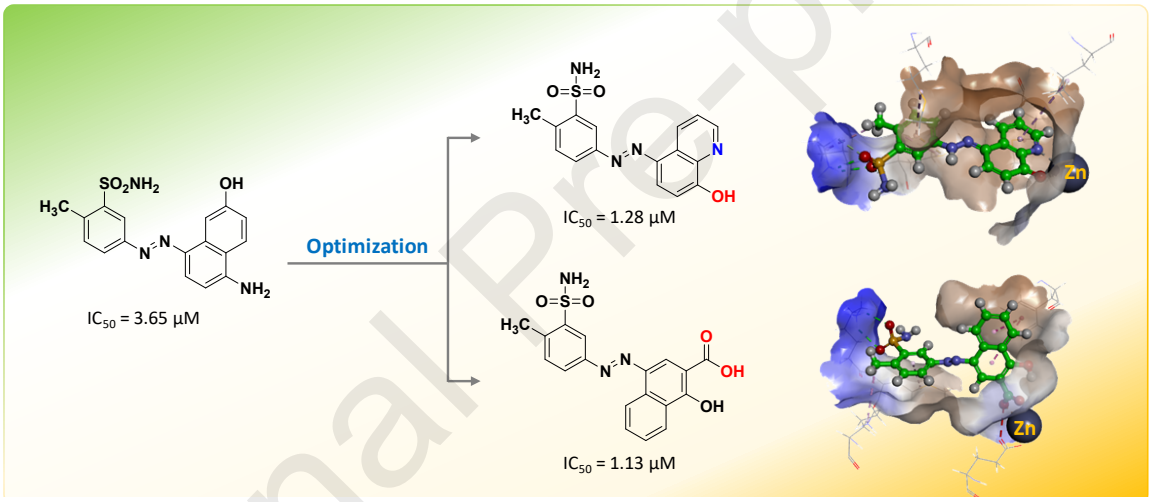

ELSEVIER

Bioorganic & Medicinal Chemistry
journal homepage: www.elsevier.com

Design, synthesis and biological evaluation of novel glyoxalase I inhibitors possessing diazenylbenzenesulfonamide moiety as potential anticancer agents

Buthina A. Al-Oudat[a,] *, Hana'a M. Jaradat[a], Qosay A. Al-Balas[a], Nizar A. Al-Shar'i[a], Amanda Bryant-Friedrich[b], Mel F. Bedi[b]

[a]*Department of Medicinal Chemistry and Pharmacognosy, Faculty of Pharmacy, Jordan University of Science and Technology, P.O. Box 3030, Irbid 22110, Jordan*
[b]*Department of Medicinal and Biological Chemistry, College of Pharmacy and Pharmaceutical Sciences, University of Toledo, Toledo, OH, 43606, USA*

* Corresponding author. Tel.: +962-775816841; fax: +962-27095123; e-mail: baoudat@just.edu.jo (Buthina A. Al-Oudat)

ARTICLE INFO

Article history:
Received
Received in revised form
Accepted
Available online

Keywords:
Anticancer agents
Glyoxalase-I
Diazenylbenzenesulfonamide
Zinc binding groups
Molecular docking

ABSTRACT

The enzyme glyoxalase-I (Glo-I) is an essential therapeutic target in cancer treatment. Significant efforts have been made to discover competitive inhibitors of Glo-I as potential anticancer agents. Herein, we report the synthesis of a series of diazenylbenzenesulfonamide derivatives, their *in vitro* evaluation against Glo-I and the resulting structure-activity relationships. Among the compounds tested, compounds **9h** and **9j** exhibited the highest activity with IC_{50} 1.28 μM and 1.13 μM, respectively. Docking studies to explore the binding mode of the compounds identified key moieties that may contribute to the observed activities. The active compounds will serve as suitable leads for further chemical optimization.

1. Introduction

Despite the enormous efforts put into cancer prevention and treatment, cancer remains a major public health problem worldwide.[1] Cancer is a rebound system of uncontrolled growth that originates in the human body from the accumulation of genetic and epigenetic changes in normal cells.[2] Cancer chemotherapeutic treatment, where chemical substances are used as anti-cancer agents, is often accompanied by toxic side effects. This is usually due to the lack of selectivity for tumor cells over normal cells. For that reason, there is a growing need for the identification of suitable druggable macromolecules that can be targeted selectively by anti-tumor agents in cancer cells. In an effort to find unique targets for anticancer agents, the glyoxalase system has been demonstrated as a plausible one.[3-4] The glyoxalase system has a detoxification function in living cells. It mediates the catalysis process of the GSH-dependent conversion of the α-oxoaldehydes such as methylglyoxal into D-lactic acid.[5-7] Methylglyoxal is a cytotoxic by-product generated from the glycolysis process during normal metabolism.[8] Its cytotoxicity is due to its ability to form adducts with cellular proteins, lipids, and nucleic acids.[9-12] The glyoxalase system consists of two enzymes, glyoxalase I (Glo-I) and glyoxalase II (Glo-II) and a catalytic amount of glutathione (GSH). In the detoxification process, the methylglyoxal **1** is converted nonenzymatically into thiohemiacetal **2**; the substrate for the Glo-I. Through the formation of ene-diolate intermediate **3**, Glo-I catalyzes the isomerization of thiohemiacetal **2** to the thioester S-D-lactoylglutathione **4** which then undergoes a catalytic hydrolysis to the non-toxic D-lactic acid **5** and reduced glutathione by Glo-II (**Figure 1**).[5, 13-14] It has been proposed that inhibition of the glyoxalase pathway in cancer cells leads to accumulation of the toxic methylglyoxal resulting in self-destruction of the cancer cells.[15]

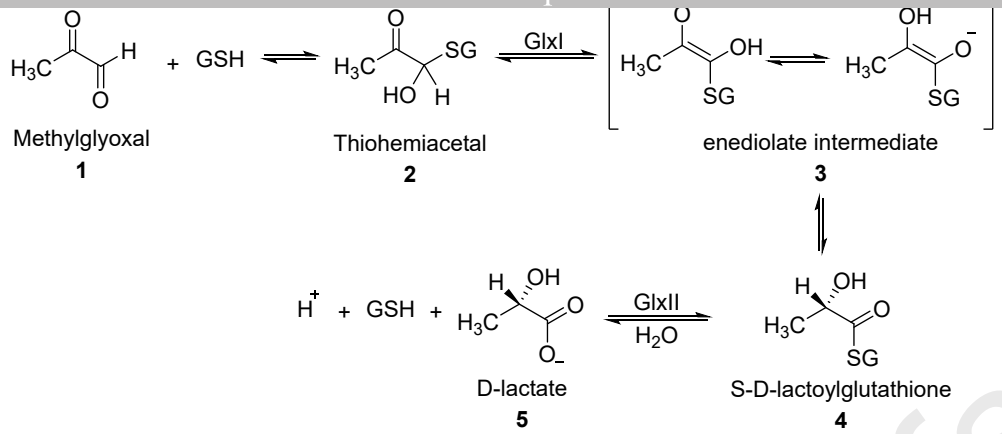

Figure 1. Normal pathway of glyoxalase enzyme system

Selective inhibition of the glyoxalase system in cancerous cells is expected to be obtained due to the increasing activity and overexpression of the enzyme in the metabolically active cancerous cells.[16-18] Among the two enzymes of the glyoxalase detoxification pathway, Glo-I has gained special attention as a promising target for the development of potential anti-cancer agents for two reasons. First, Glo-I drives the rate- limiting step of the detoxification biological process. Second, Glo-I overexpression was associated with multidrug resistance of a wide variety of tumors suchlike monocytic leukemia and erythro leukemia.[19-20] Potent and selective inhibition of Glo-I in cancerous cells would therefore induce elevated concentration of the cytotoxic methylglyoxal leading to apoptosis of tumor cells.

Structurally, the human Glo-I is a homodimeric mononuclear zinc metalloenzyme with each monomer consisting of 184 amino acids and a mass of 42 kDa.[21] It has been determined that the Glo-I active site can be divided into three main regions, namely a positively charged entrance (Arg37, Arg122, and Lys156), a central zinc atom which is involved in stabilizing the enediolate intermediate, and a deep hydrophobic pocket (Phe62, Leu69, Leu92, and Met179).[22]

In the past decades there have been extensive efforts to identify and design potent Glo-I inhibitors with structural diversity and a range of different inhibitory activities utilizing different drug discovery methodologies.[23] Substrate and transition-state analogues were among the first class of compounds designed as competitive Glo-I inhibitors.[3, 24-26] Natural products and natural product derivatives were utilized as another approach to obtain such inhibitors.[27-30] Recent studies have utilized different approaches to identify new Glo-I inhibitors including high-throughput screening[31-32] and *in silico* computer aided drug design.[29, 33-35] Recently, Al-Sha'er *et al.* utilized a structure-based pharmacophore approach to obtain a pharmacophore model for the Glo-I active site.[36] Ninety two pharmacophore models were generated utilizing eighteen co-crystallized protein-ligand structural complexes. Subsequent QSAR modeling followed by ROC evaluation identified a single pharmacophore model called Hypo (3VW9) which was able to predict the expected Glo-I inhibition. Hypo (3VW9) was used to screen compounds in the National Cancer Institute (NCI) database that resulted in the identification of several promising hits. The hit compounds were purchased and subjected to experimental biochemical assay that led to the identification of seven hits with IC_{50} at the low micromolar range. Herein, one of the hits was used as a lead compound to develop more potent inhibitors of Glo-I. The selected hit possesses diazenylbenzenesulfonamide moiety, exhibited IC_{50} value equal to 3.65 µM. The structure of the selected hit is shown in **Figure 2**. In the present study, structural analogues of the hit compound **6** were proposed based on their synthetic feasibility and the pivotal chemical features that are required for optimal inhibitor binding to the active site. Three chemical features can be utilized to assure better inhibitor binding to the active site of the enzyme including; a zinc binding group to chelate the zinc atom at the center of the active site, a negatively ionizable group for binding to the positively ionized active site mouth and a hydrophobic group that can accommodate the deep hydrophobic pocket of the enzyme. The proposed compounds were synthesized and biologically evaluated *in vitro* against human Glo-I enzyme. Structure-activity relationships were obtained through structural manipulations of the synthesized analogues. Docking studies were performed on the most active compounds to explore the binding modes of these compounds at the active site.

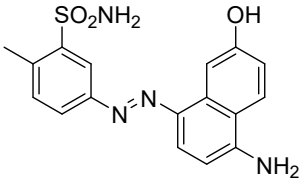

6

Figure 2. Structure of obtained hit with IC_{50} equal to 3.65 µM.[36]

2. Results and discussion

2.1. Chemistry

To discover and develop competitive inhibitors of Glo-I as potential anticancer drugs, we report here the preparation of a series of compounds (**9a-x**) that are structurally related to the lead compound **6**. The synthetic routes adopted for the synthesis of all target compounds are outlined in **Scheme 1**. The syntheses utilized a set of different structures of commercially available starting materials containing aromatic amino moiety (**7** or **10**) that were subjected to diazotization reactions yielding diazonium salt intermediates (**8** or **11**) which then were coupled with

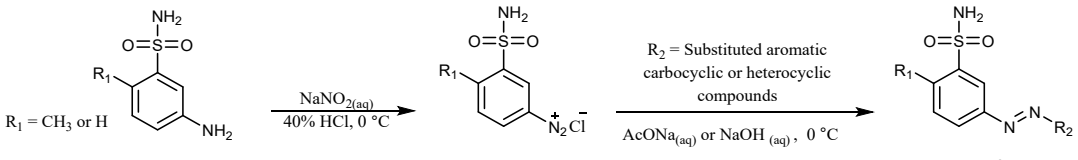

7 **8** **9a-q**

Scheme 1. Synthesis of the target compounds **9a-x.**

different structures of substituted aromatic carbocyclic and heterocyclic compounds.[37] We have chosen various R moieties (R_1, R_2 and R_3) to be present in the derivatives **9a-x** including: polar moieties such as sulfonamide, hydroxyl and amino groups, ionizable moieties such as carboxylic and sulfonic acid groups, and hydrophobic moieties such as benzene and naphthalene groups. Besides the above mentioned ionizable and polar groups, 8-hydroxyquinoline, 2-hydroxybenzoic acid and 2-hydroxynaphthoic acid moieties were included in the derivatives as they were presumed to chelate with the zinc ion of the enzyme and/or form hydrogen bond interactions with the target protein which should be highly beneficial for the inhibitory activity of the compounds. The identities of all the synthesized compounds were confirmed by ^{1}H-NMR, ^{13}C NMR and high resolution (HR)-MS. All the target compounds are listed in Table **1** and Table **2**.

2.2. Glo-I Inhibition, SAR study and Molecular docking

The lead compound **6** has been previously reported as Glo-I inhibitor with IC_{50} value equal to 3.65 μM.[36] Herein, structure–activity relationship (SAR) studies around this lead compound resulted in the identification of a series of analogues that demonstrated a broad range of inhibition (low μM to inactive) as shown in Table **1** and Table **2**. Structurally, compound **6** has the diazenyl-2-methylbenzenesulfonamide moiety attached to position 8 of the 2-hydroxy-5-aminonaphthalene moiety. The SAR studies were started through investigating the importance of the identity and position of the substituents on the naphthalene moiety of compound **6** through the synthesis of compounds **9a-9c**. Moving the hydroxyl group of compound **6** from position 2 to position 3 or 1 (compounds **9a** or **9b**) led to moderate or significantly reduced inhibitory activity, respectively. Removing the hydroxyl group from the naphthalene moiety produced a totally inactive compound (compound **9c**). On the other hand, attaching the diazenyl-2-methylbenzenesulfonamide moiety to position 1 of the 2-hydroxynaphthalene resulted in compound **9d** with weak inhibitory activity. Introducing an amino group to position 8 in compound **9d** led compound **9e** with moderate inhibitory activity. These results reveal that the hydroxyl group at position 2 and the amino group at position 5 of the naphthalene ring are important for the inhibitory activity of compound **6**. At this point, we decided to modify compound **6** through replacing the 2-hydroxy-5-aminonaphthalene moiety with functional groups that have the potential to chelate the zinc ion of the enzyme and/or form hydrogen bond interactions with amino acid residues within the active site in order to enhance the inhibitory activity of the compounds. For that reason, compounds **9f-9k** were synthesized. Inclusion of a 2-hydroxy-1-naphthaldehyde (compound **9f**) or a 7-hydroxy-2H-chromen-2-one (compound **9g**) moieties led to moderate inhibitory activities. Interestingly, inclusion of 8-hydroxyquinoline moiety provided compound **9h** with IC_{50} value of 1.28 μM. Selection of the 8-hydroxyquinoline moiety was based on a reported Glo-I inhibitor (compound **12**, Figure **3**) which was developed with a novel sulfonamide core pharmacophore exhibiting IC_{50} 0.46 μM.[35] It has been demonstrated that compound **12** binds the catalytic zinc ion of Glo-I in a bidentate fashion through the endocyclic nitrogen and exocyclic sulfonamide-nitrogen donor atoms (in red). Here, we propose that similar interactions with the zinc ion were attained by the 8-hydroxyquinoline moiety in compound **9h** utilizing the endocyclic nitrogen and exocyclic hydroxyl-oxygen functionalities (in red). To investigate the binding modes of the synthesized compounds, particularly compound **9h**, within the binding site of Glo-I, we performed molecular docking using CDOCKER algorithm within Discovery Studio (DS) software. The best predicted docked pose for compound **9h** in addition to its 2D interaction map with active site residues are shown in **Figure 4**, which explains the good activity of the compound. The docked pose showed that the 8-hydroxyquinoline moiety coordinated with the Zn ion in a bidentate fashion through the endocyclic nitrogen and exocyclic hydroxyl-oxygen donor atoms of the tautomerized form of the compound. Moreover, the sulfonamide group contributed to the compound potency through providing hydrogen bond interactions with Lys156 and Met157, whereas the aromatic rings enhanced the compound's activity through providing binding interactions with the hydrophobic region of the enzyme including Met65, Met179 and Leu69.

On the other hand, it was reported that the Glo-I inhibitor (compound **13**, Figure **3**) that possesses di-salicylic acid moieties exhibits good Glo-I inhibitory activity with IC_{50} 0.34 μM.[38] It has been shown that the activity of this compound is due to the ability of the ionizable di-salicylic acid moiety to form strong interactions with the zinc ion, Arg37 and Arg122 at the active site of the enzyme. For that reason, 2-hydroxybenzoic acid moiety was used to produce compound **9i** (IC_{50} 11.5 μM) that was optimized through introducing another fused benzene ring (hydroxynaphthoic acid) which gave compound **9j** that was found to be the most active among the synthesized compounds with IC_{50} 1.13 μM. The binding mode of compound **9j** within Glo-I is depicted in Figure **4**. The docked pose showed the importance of the ionizable carboxylic moiety to the activity of the compound due to its ability to form a metal-acceptor coordination and an electrostatic interaction with the zinc ion. Moreover, the docked pose showed that the sulfonamide group provided significant hydrogen bond interactions with Lys156 and Met157. In addition, the hydrophobic aromatic benzene and naphthalene moieties stabilized the compound in the active site

thro ...hese enzyme (Phe67 and Lys150). An attempt to further optimize compound **9j** through changing the position of the carboxyl and hydroxyl groups, as shown in compound **9k**, led to significant reduction in activity producing totally inactive compound. This key functional groups seen in compound **9j**, which upon changing their positions as seen in compound **9k** had resulted in detrimental steric clashes within the active site rendering the compound completely inactive.

Table 1: The structures and inhibitory activities of the target compounds **9a-q**

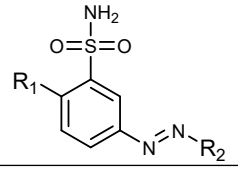

No.	R_1	R_2	- CDOCKER Energy (Kcal/mol)	% Inhibition at 25 µM	IC_{50}[a] (µM)
6	CH_3	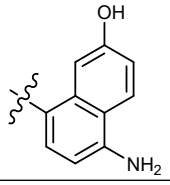	27.59	76.43	3.65
9a	CH_3	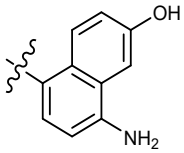	32.8617	57.2	18.90 ± 0.52
9b	CH_3	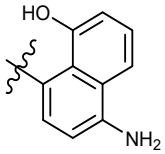	28.4877	ND	>100
9c	CH_3	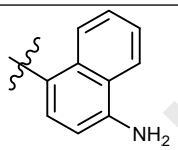	17.5752	24.74	95.70 ± 12.2
9d	CH_3	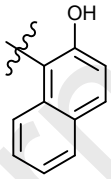	18.675	34.45	45.02 ± 1.95
9e	CH_3	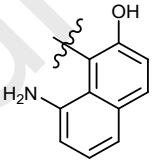	24.7535	54	24.00 ± 2.41
9f	CH_3	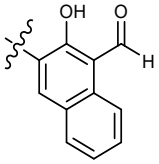	34.6445	57.36	18.57 ± 0.10
9g	CH_3	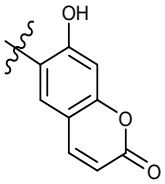	35.3771	58.98	17.81 ± 0.08

9h	CH_3	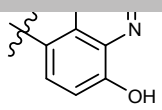	33.7361	92.14	1.28 ± 0.12
9i	CH_3	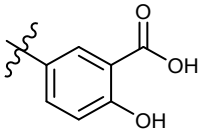	51.033	67.72	11.48 ± 0.45
9j	CH_3	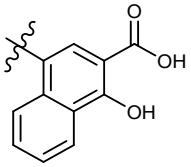	41.0963	100	1.13 ± 0.06
9k	CH_3	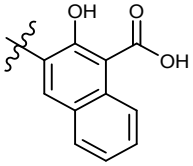	39.7131	ND	>100
9l	H	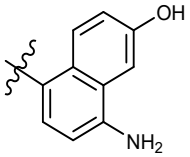	41.3362	66.04	21.83 ± 0.24
9m	H	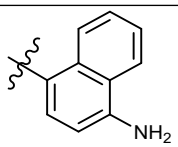	20.0072	28.096	85.81 ± 10.32
9n	H	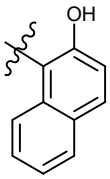	20.0229	39.04	37.51 ± 0.42
9o	H	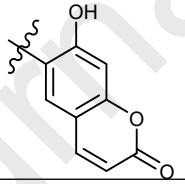	36.5897	64.36	18.95 ± 0.37
9p	H	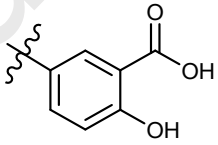	55.1658	76.47	8.66 ± 0.12
9q	H	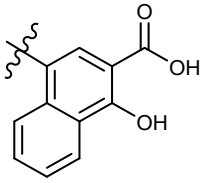	48.4885	96.54	1.22 ± 0.07
Myricetin			-	-	3.38 ± 0.41

[a] The IC_{50} values are represented as the mean ± standard error of the mean of three independent experiments performed in triplicate.

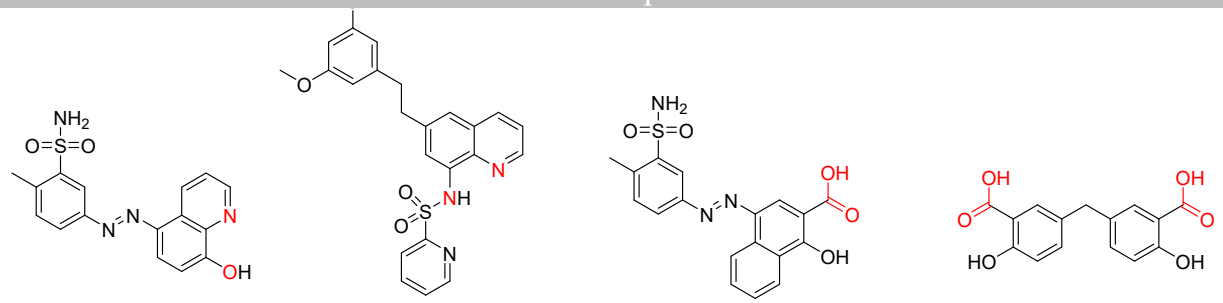

9h

IC_{50} = 1.28 μM
(**This work**)

12

IC_{50} = 0.46 μM

9j

IC_{50} = 1.13 μM
(**This work**)

13

IC_{50} = 0.34 μM

Figure 3. Molecular structures of previously reported Glo-I inhibitors with corresponding IC_{50} values. Metal binding atoms are highlighted in red.

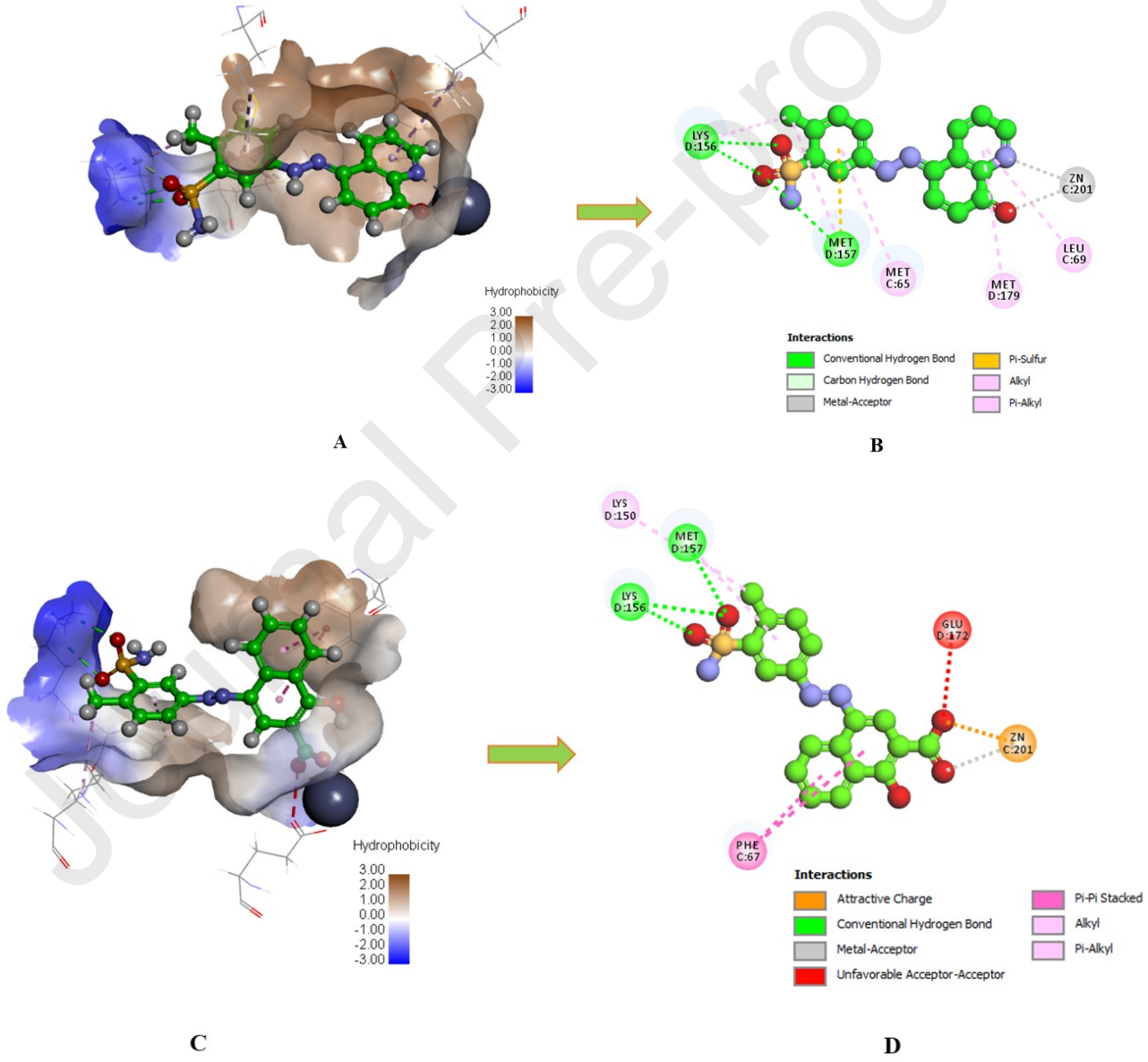

Figure 4. A. A 3D representation of the docked pose of compound **9h** within the active site of the Glo-I enzyme (PDB code 3W0T (resolution of 1.35 Å)). The binding site is represented as a hydrophobic surface (blue is positively charged areas and brown is hydrophobic areas), docked compounds are shown in balls and sticks with carbons colored green, and the Zn^{2+} ion as a grey sphere. **B.** A 2D interaction map showing the different interactions between compound **9h** and the active site of the enzyme. Residues are colored according to the type of their interactions with the ligand, the interactions are shown as dashed lines. **C**. A 3D

repre map showing the different interactions between compound **9j** and the active site of the enzyme.

Then, we investigated the importance of the methyl group at position [illegible] synthesis of compounds **9i-9q.** The SAR study showed that the analogues lacking the methyl group exhibited similar activities as the methyl-containing analogues. This may be attributed to the small size of the methyl moiety which may have no influence on the binding modes of the inhibitors with the target enzyme.

Next, we decided to explore the SAR for one of the most active analogues (compound **9h)** in order to identify the important binding groups that provide the critical binding [illegible] end, additional synthetic efforts were made to obtain compounds **9r-9x** (**Table 2**). Moreover, molecular docking of these compounds into the Glo-I active site was performed to give an explanation and understanding of the activity observed providing an insight for structural interpretation of SAR (**Figure 5** and **Figure 6**).

Table 2: Structural modifications on compound **9h**

No.	Structure	- CDOCKER Energy (Kcal/mol)	% Inhibition at 25 µM	IC_{50}[a] (µM)
9h	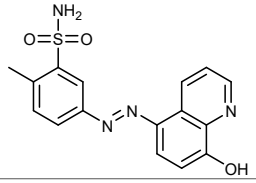	33.7361	92.14	1.28 ± 0.12
9r	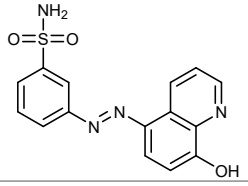	33.0826	98.28	1.36 ± 0.09
9s	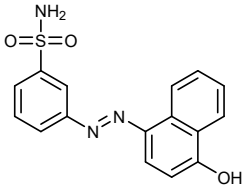	26.1108	38.31	52.19± 0.72
9t	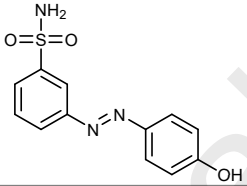	35.5576	59.91	13.36 ± 0.53
9u	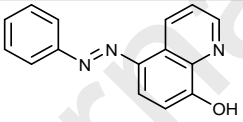	21.8737	82.78	9.13 ± 0.044
9v	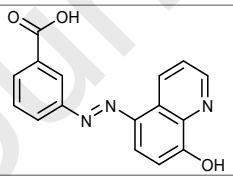	38.8429	90.71	4.37 ± 0.43
9w	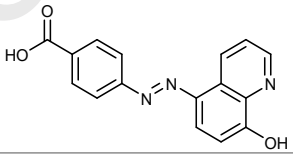	38.0737	79.87	4.45 ± 0.30
9x	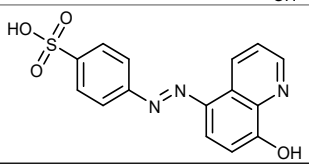	14.7322	74.99	9.70 ± 0.06

[a] The IC_{50} values are represented as the mean ± standard error of the mean of three independent experiments performed in triplicate.

Compound **9r** that lacks the methyl group at position 2 of the benzenesulfonamide moiety exhibited similar activity to compound **9h**, which is supported by the 2D interaction map that displayed similar binding interactions to compound **9h** (**Figure 5**). This result confirms the insignificant role of the methyl group in the binding mode with the target enzyme as previously observed in compounds **9l-9q**. To investigate the importance of the pyridine-nitrogen atom to the activity of compound **9h**, compound **9s** that lacks the nitrogen atom was synthesized which was found to have weak inhibitory activity. The significant reduction in the inhibitory activity of **9s** may be attributed to the mono-chelation of the zinc ion to the hydroxyl group in contrast to the di-chelation to the endocyclic pyridine-nitrogen and exocyclic hydroxyl-oxygen donor atoms of the 8-hydroxyquinoline moiety, as shown by the 2D interaction maps (**Figure 5**). These results suggest that the pyridine-nitrogen atom greatly contributes to the Glo-I inhibitory activity of compound **9h**. In contrast to compound **9s**, total removal of the pyridine moiety (compound **9t**, IC_{50} = 13.36 µM) led only to small decrease in activity, when compared to compound **9h**, which can be explained through the analysis of its binding mode within the active site. The 2D interaction map of compound **9t** shows that the compound flips over in the enzyme active site allowing the formation of several binding interactions with the amino acid residues at the active site of the enzyme (**Figure 5**). The hydroxyl group of the phenol moiety interacts with Lys156 while the sulfonamide moiety interacts with the zinc ion, Glu172 and His126. We propose that these binding interactions compensated for the loss of binding interactions provided by the pyridine ring.

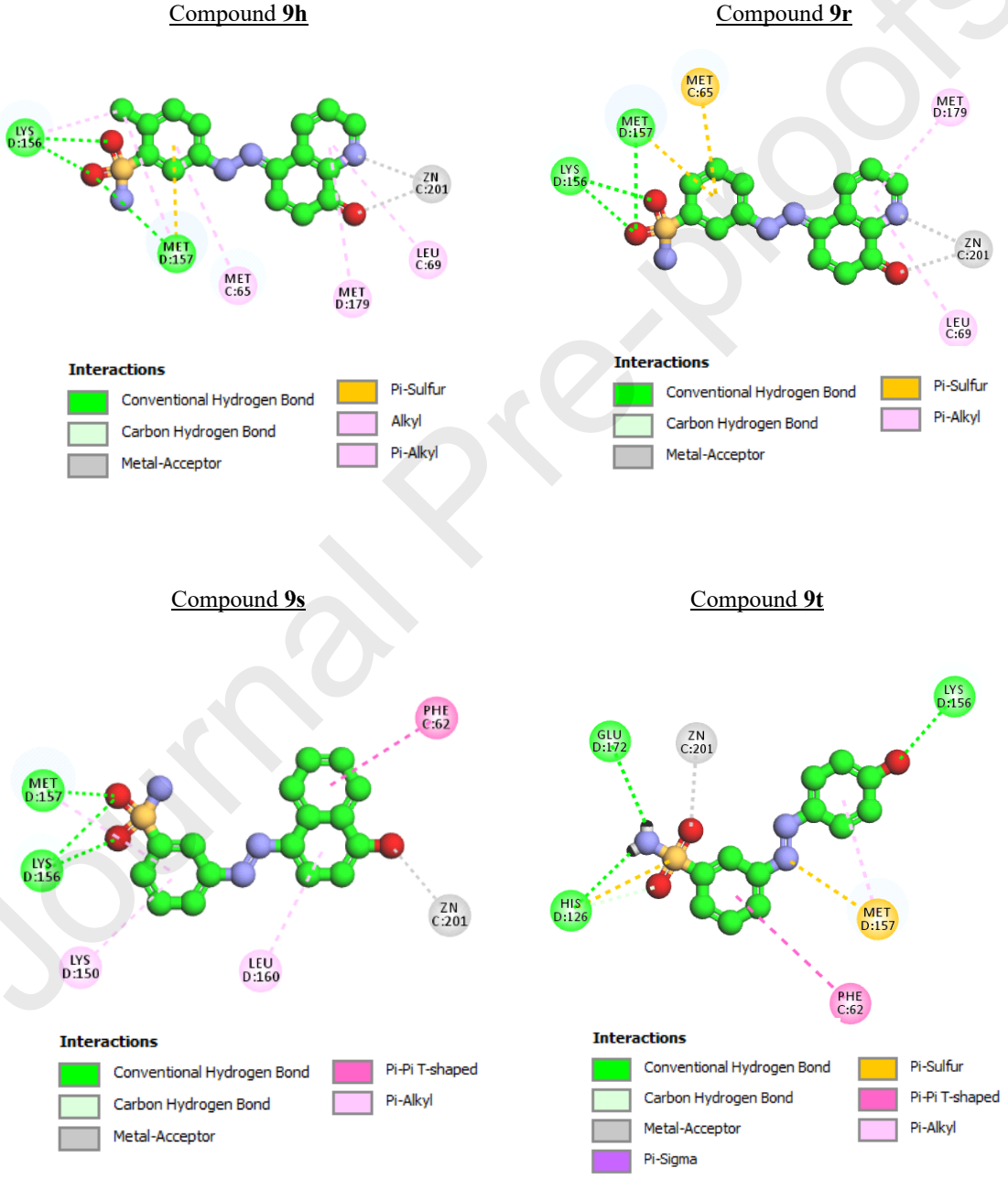

Figure 5. 2D interaction maps of compounds **9h**, **9r-9t** showing the types of different interactions they establish with key amino acids within Glo-I active site.

Next, we decided to investigate the importance of the sulfonamide moiety to the activity of compound **9h** through the synthesis of compound **9u**. As predicted, this modification resulted in some loss in the inhibitory activity leading to moderately active compound (IC_{50} = 9.13 µM). Keeping some of the potency for compound **9u** may be attributed to the binding

interaction di-chelation of the Zn ion to the endocyclic pyridine-nitrogen and exocyclic hydroxyl-oxygen donor as well as the extra hydrophobic interactions by the benzene ring with Met65 and Met157, as shown by the 2D interaction map (**Figure 6**). Isosteric replacement of the sulfonamide moiety with a carboxyl group, produced compound **9v** with IC_{50} value of 4.37 µM. The di-chelation interactions of the zinc ion to the 8-hydroxyquinoline moiety as well as the ionic bonds with Lys150 and Lys156 and hydrogen bond interaction with Lys156 by the carboxyl group contributed to the potency of compound **9v**. relative to the diazinyl group generated compound **9w** (IC_{50} 4.45 µM) with similar activity to compound **9v**. Replacement of the sulfonamide moiety with a sulfonate group produced moderately active compound (**9x**) with IC_{50} value of 9.7 µM. Although this highly acid functionality was anticipated to enhance the binding affinity, hence the overall activity, the observed activity could be attributed to solubility issues, since this compound was the least soluble under the used assay conditions. The 2D interaction maps of compounds **9v-9x** are shown in figure **6**.

Compound **9u**

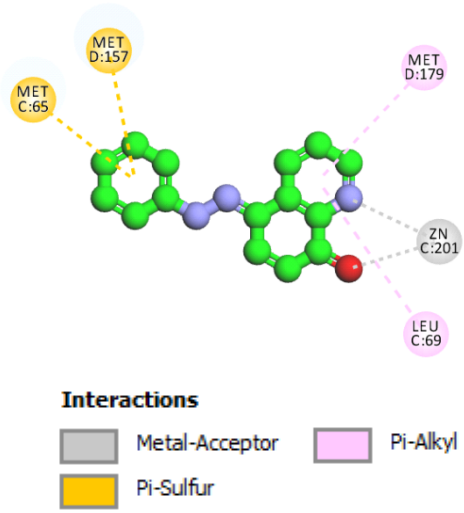

Compound **9v**

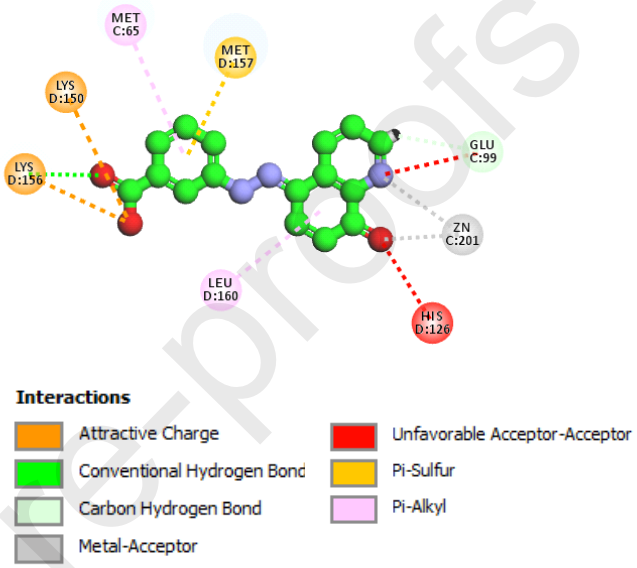

Compound **9w**

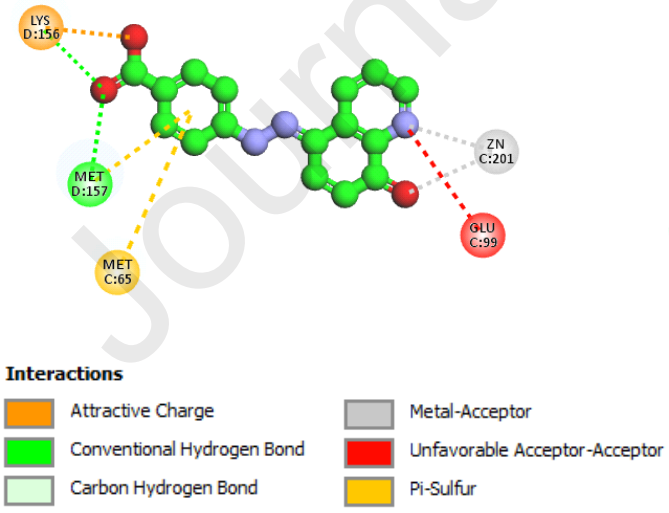

Compound **9x**

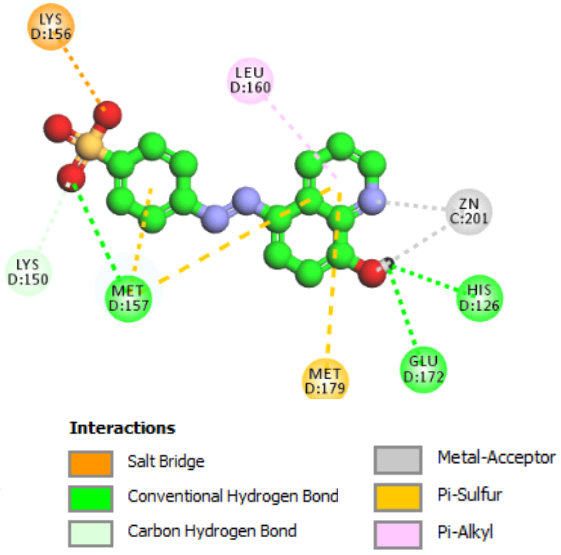

Figure 6. 2D interaction maps of compounds **9u-9x** showing the types of different interactions they establish with key amino acids within Glo-I active site.

Given the high cost of drug discovery and development processes, it is highly recommended to direct and focus efforts towards lead compounds with favorable ADMET properties and eliminate ones that could lead to later problems due to unfavorable ADMET characteristics. Therefore, we calculated the ADMET descriptors and Toxicity parameters for compounds that showed promising Glo-I inhibitory activities in order to guide future lead optimization. ADMET refers to the Absorption, Distribution, Metabolism, Excretion, and Toxicity properties of a molecule within an organism.

The *ADMET Descriptors* protocol in DS was used to calculate a range of ADMET related properties including, aqueous solubility (AS), blood brain barrier (BBB) penetration, CYP2D6 inhibition, hepatotoxicity, human intestinal absorption (HIA), plasma protein binding (PPB), AlogP, and polar surface area (PSA). In addition, different toxicity parameters were also calculated using the *Toxicity Prediction (TOPKAT)* protocol in DS. The calculated toxicity parameters were rodent carcinogenicity (for both male and female rats), Ames mutagenicity (AM), skin irritation (SI), ocular irritancy (OI), aerobic biodegradability and developmental toxicity potential (AB) (**Table 3**, **Supplementary Material**). Based on the calculated values, particularly mutagenicity and carcinogenicity, compounds **9j** and **9q** show promising ADMET and toxicity profiles, and as we show above, these compounds also showed the highest activity.

3. Conclusions

In summary, a series of novel diazenylbenzenesulfonamide derivatives were synthesized and evaluated *in vitro* against Glo-I enzyme. Structural modification of compound **6** produced several derivatives that exhibited inhibitory activity with IC_{50} values in the low micromolar range. Replacing the 2-hydroxy-5-aminonaphthalene moiety of compound **6** with 8-hydroxyquinoline moiety provided compound **9h** with IC_{50} 1.28 µM. SAR analysis of compound **9h** revealed the importance of the nitrogen atom and hydroxyl group of the 8-hydroxyquinoline moiety as well as the sulfonamide moiety in exerting the inhibitory activity of the compound. Isosteric replacement of the sulfonamide moiety with a carboxyl group produced active compounds with comparable potency to compound **9h** with IC_{50} values less than 5 µM. On the other hand, hydroxynaphthoic acid moiety in compound **9j** was proved to be an exceptional replacement for the 2-hydroxy-5-aminonaphthalene moiety of compound **6** as it was found that compound **9j** (IC_{50} 1.13 µM) is the most active among the synthesized compounds. Docking studies of these active compounds into Glo-I active site provided the probable binding modes and thus highlighted the important functional groups that have the potential to chelate the zinc ion of the enzyme and/or form hydrogen bond interactions with the polar amino acid residues within the active site as well as the hydrophobic groups that can accommodate the deep hydrophobic pocket of the enzyme. Lastly, the calculated toxicity profile of **9j** also supports this compound as a lead worthy of further investigation

4. Experimental Section

4.1. Chemistry

All reagents and solvents were obtained from commercial sources and used without further purification. Reaction's progress was qualitatively analyzed by thin-layer chromatography (TLC) using 0.25 mm E. Merck silica gel plates (60 F-254, 0.2 mm). Merck silica gel 60 was used for column chromatography. Compound spots were visualized by UV light (254 nm). $^{1}H/^{13}C$ NMR spectra were recorded at ambient temperature on a Bruker AVANCE 400 MHz or 600 MHz instruments. The spectra were obtained in ppm using automatic calibration to the residual proton peak of the solvent, DMSO-d_6. The ^{1}H NMR data are presented as follows: chemical shift (δ ppm), multiplicity (s = singlet, d = doublet, dd = doublet of doublet, t = triplet, q = quartet, m = multiplet), coupling constants (Hz), and integration. The ^{13}C NMR analyses were reported in terms of chemical shift. High resolution mass spectra were acquired using Waters Synapt HDMS (ESI Q-TOF MS) equipped with nanoAcquity UPLC system and traveling wave ion mobility MS in the College of Arts and Sciences and Mathematics Instrumentation Center at the University of Toledo, 2801 W Bancroft drive, Toledo, OH, USA.

4.1.1 General procedure for the synthesis of target compounds 9a-9x.

The synthesis of the target compounds was achieved according to published literature procedures with some modifications utilizing the following two steps.[37]

Step 1: Preparation of diazonium chloride solutions of aromatic amines: The aromatic amine-containing compound (0.20 g, 1.0 eq) was dissolved in a freshly prepared 40% solution of concentrated hydrochloric acid in de-ionized water (3 ml) then cooled down to -5 ºC in ice/sodium chloride path. To that was added dropwise an aqueous solution of $NaNO_2$ (1.2 eq, 2M). Then the reaction mixture was kept stirring at the same temperature for 15 min to produce the diazonium chloride solution which is required for the next step. The solution was freshly prepared prior to use.

Step 2: Diazo coupling of the diazonium chloride solutions with substituted aromatic carbocyclic and heterocyclic compounds:

Method A:

The solution of diazonium chloride (prepared in step 1) was added dropwise to a solution of a substituted aromatic carbocyclic or heterocyclic compound (1.0 equiv.) in a saturated aqueous solution of sodium acetate (3.0 ml) at -5 ºC. Upon reaction completion, the mixture was warmed to room temperature and the pH was adjusted to 7. The solid was collected by filtration, washed with a minimum amount of deionized H_2O, air dried and purified by silica gel column chromatography eluting with 5% MeOH in DCM to give the desired compounds in good yields.

Method B: In this method, similar procedure as in method A was used to synthesize the target compounds except in method B sodium hydroxide was used as a base instead of sodium acetate.

4.1.1.1. (E)-5-((4-amino-6-hydroxynaphthalen-1-yl)diazenyl)-2-methylbenzenesulfonamide (9a). The product was obtained as a dark purple solid using method A. Yield (79%). ^{1}H NMR (400 MHz, DMSO-d_6): δ 8.60 (d, J = 9.0 Hz, 1H), 8.30 (d, J = 9.2 Hz, 1H), 8.25 (s, 1H), 7.90 (d, J = 8.2 Hz, 1H), 7.60-7.58 (m, 3H), 7.48 (d, J = 8.2 Hz, 1H), 7.39 (d, J = 9.0 Hz, 1H), 7.08 (d, J = 9.2 Hz, 1H), 2.61 (s, 3H). ^{13}C NMR (DMSO-d_6): δ 156.95, 143.66, 143.26, 133.95, 133.47, 128.08, 125.28, 123.36, 122.81, 120.83, 116.33, 107.32, 19.53. HRMS (ESI, m/z): calculated for $C_{17}H_{17}N_4O_3S$ $[M+H]^+$ 357.1016; found 357.1013.

4.1.1.2. (E)-5-((4-amino-8-hydroxynaphthalen-1-yl)diazenyl)-2-methylbenzenesulfonamide (9b). The product was obtained as purple solid using method A. Yield (44%). ^{1}H NMR (400 MHz, DMSO-d_6): δ 12.38 (s, 1H), 8.19-8.15 (m, 2H), 7.71 (m, 2H), 7.56 (m, 4H), 7.35 (t, J = 8.0 Hz, 1H), 7.06 (d, J = 7.2 Hz, 1H), 6.82 (d, J = 8.8 Hz, 1H), 2.66 (s, 3H). ^{13}C NMR (DMSO-d_6): δ 155.75, 153.48, 150.10, 143.40, 138.38, 136.67, 133.72, 125.57, 123.47, 122.24, 120.25, 120.14, 117.09, 114.13, 113.88, 109.29, 19.76. HRMS (ESI, m/z): calculated for $C_{17}H_{17}N_4O_3S$ $[M+H]^+$ 357.1016; found 357.1013.

4.1.1.3. (E)-5-((4-aminonaphthalen-1-yl)diazenyl)-2-methylbenzenesulfonamide (9c). The product was obtained as black solid using method B. Yield (53%). ^{1}H NMR (400 MHz, DMSO-d_6): δ 8.76 (d, J = 8.3 Hz, 1H), 8.46 (d, J = 8.0 Hz, 1H), 8.39 (d, J = 8.3 Hz, 1H), 8.32 (s, 1H), 7.97 (d, J = 8.0 Hz, 1H), 7.79 (t, J = 7.5 Hz, 1H), 7.63-7.48 (m, 4H), 7.07 (d, J = 9.2 Hz, 1H), 2.62 (s, 3H). ^{13}C NMR (DMSO-d_6): δ 151.44, 150.59, 143.18, 136.40, 136.26, 133.50, 133.28, 127.98, 124.96, 124.67, 122.84, 122.70, 121.13, 119.50, 116.20, 108.12, 19.75. HRMS (ESI, m/z): calculated for $C_{17}H_{17}N_4O_2S$ $[M+H]^+$ 341.1067; found 341.1046.

4.1.1.4. (E)-5-((2-hydroxynaphthalen-1-yl)diazenyl)-2-methylbenzenesulfonamide (9d). The product was obtained as orange solid using method B. Yield (41%). ^{1}H NMR (400 MHz, DMSO-d_6): δ 15.51 (s, 1H), 8.56 (d, J = 8.1 Hz, 1H), 8.34 (s, 1H), 7.99 (d, J = 8.9 Hz, 2H), 7.81 (d, J = 7.8 Hz, 1H), 7.66-7.63 (m, 3H), 7.55 (d, J = 8.1 Hz, 1H), 7.48 (t, J = 7.3 Hz, 1H), 6.97 (d, J = 9.3 Hz, 1H), 2.65 (s, 3H). ^{13}C NMR (DMSO-d_6): δ 167.16, 143.74, 143.61, 139.89, 135.75, 133.74, 132.57, 129.38, 129.13, 128.95, 127.98, 125.96, 123.40, 122.55, 121.30, 117.13, 19.66. HRMS (ESI, m/z): calculated for $C_{17}H_{16}N_3O_3S$ $[M+H]^+$ 342.0907; found 342.0910.

4.1.1.5. (E)-5-((8-amino-2-hydroxynaphthalen-1-yl)diazenyl)-2-methylbenzenesulfonamide (9e). The product was obtained as dark purple solid using method B. Yield (23%). ^{1}H NMR (600 MHz, DMSO-d_6): δ 7.97 (s, 1H), 7.81 (dd, J = 9.6, 2.6 Hz, 1H), 7.57 (d, J = 8.1 Hz, 1H), 7.52 (s, 2H), 7.48 (dd, J = 8.2, 2.1 Hz, 1H), 7.22 (td, J = 7.9, 2.7 Hz, 1H), 7.16 (s, 2H), 7.09 (d, J = 8.1 Hz, 1H), 6.99 (d, J = 7.2 Hz, 1H), 6.65 (dd, J = 9.6, 2.6 Hz, 1H), 2.59 (s, 3H). ^{13}C NMR (DMSO-d_6): δ 181.66, 145.85, 145.01, 143.50, 140.17, 134.05, 133.83, 131.74, 129.48, 127.43, 125.50, 119.21, 118.72, 118.47, 113.88, 112.41, 19.30. HRMS (ESI, m/z): calculated for $C_{17}H_{17}N_4O_3S$ $[M+H]^+$ 357.1016; found 357.1026.

4.1.1.6. (E)-5-((4-formyl-3-hydroxynaphthalen-2-yl)diazenyl)-2-methylbenzenesulfonamide (9f). The product was obtained as red solid using method B. Yield (14%). ^{1}H NMR (600 MHz, DMSO-d_6): δ 8.58 (d, J = 8.4 Hz, 1H), 8.35 (s, 1H), 8.01 (d, J = 9.0 Hz, 2H), 7.84 (d, J = 7.8 Hz, 1H), 7.67-7.64 (m, 3H), 7.56 (d, J = 7.8 Hz, 1H), 7.50 (t, J = 7.8 Hz, 1H), 6.99 (d, J = 9.0 Hz, 1H), 2.65 (s, 3H). ^{13}C NMR (DMSO-d_6): δ 166.98, 143.75, 143.60, 139.85, 135.74, 133.69, 132.53, 129.33, 129.10, 128.94, 127.96, 125.92, 123.35, 122.62, 121.27, 117.04, 19.61. HRMS (ESI, m/z): calculated for $C_{18}H_{16}N_3O_4S$ $[M+H]^+$ 370.0856; found 370.0918.

4.1.1.7. (E)-5-((7-hydroxy-2-oxo-2H-chromen-6-yl)diazenyl)-2-methylbenzenesulfonamide (9g). The product was obtained as brown solid using method B. Yield (79%). ^{1}H NMR (400 MHz, DMSO-d_6): δ 11.65 (s, 1H), 8.41 (s, 1H), 8.12-8.07 (m, 3H), 7.62-7.59 (m, 3H), 7.02 (s, 1H), 6.36 (d, J = 9.2 Hz, 1H), 2.69 (s, 3H).^{13}C NMR (DMSO-d_6): δ 159.68, 158.63, 157.17, 149.53, 144.67, 143.26, 139.41, 136.52, 133.49, 125.49, 121.44, 120.09, 113.33, 112.00, 104.49, 19.91. HRMS (ESI, m/z): calculated for $C_{16}H_{14}N_3O_5S$ $[M+H]^+$ 360.0649; found 360.0659.

4.1.1.8. (E)-5-((8-hydroxyquinolin-5-yl)diazenyl)-2-methylbenzenesulfonamide (9h). The product was obtained as brown solid using method B. Yield (92%). ^{1}H NMR (400 MHz, DMSO-d_6): δ 9.64 (d, J = 8.4 Hz, 1H), 9.11 (m, 1H), 8.44 (s, 1H), 8.14-8.02 (m, 3H), 7.66-7.61 (m, 3H), 7.48 (d, J = 8.6 Hz, 1H), 2.69 (s, 3H). ^{13}C NMR (DMSO-d_6): δ 154.70, 150.03, 146.37, 143.40, 139.14, 138.87, 137.83, 133.49, 131.60, 128.08, 125.19, 123.63, 121.26, 116.78, 114.72, 19.92. HRMS (ESI, m/z): calculated for $C_{16}H_{15}N_4O_3S$ $[M+H]^+$ 343.0859; found 343.0863.

4.1.1.9. (E)-2-hydroxy-5-((4-methyl-3-sulfamoylphenyl)diazenyl)benzoic acid (9i). The product was obtained as yellow solid using method B. Yield (43%). ^{1}H NMR (400 MHz, DMSO-d_6): δ 8.33 (d, J = 9.2 Hz, 2H), 8.10 (d, J = 8.8 Hz, 1H), 7.99 (d, J = 8.0 Hz, 1H), 7.59 (m, 3H), 7.17 (d, J = 9.2 Hz, 1H), 2.67 (s, 3H). ^{13}C NMR (DMSO-d_6): δ 171.37, 163.89, 149.69, 144.43, 143.32, 139.04, 133.56, 129.05, 126.08, 120.23, 118.59, 113.87, 19.92. HRMS (ESI, m/z): calculated for $C_{14}H_{14}N_3O_5S$ $[M+H]^+$ 336.0649; found 336.0631.

4.1.1.10. (E)-1-hydroxy-4-((4-methyl-3-sulfamoylphenyl)diazenyl)-2-naphthoic acid (9j). The product was obtained as dark red solid using method B. Yield (85%). ^{1}H NMR (400 MHz, DMSO-d_6): δ 8.91 (d, J = 8.4 Hz, 1H), 8.46 (d, J = 1.6 Hz, 1H), 8.41 (d, J = 8.0 Hz, 1H), 8.26 (s, 1H), 8.17 (d, J = 8.0, 1.6 Hz, 1H), 7.91 (t, J = 7.6 Hz, 1H), 7.75 (t, J = 7.6 Hz, 1H), 7.63 (m, 3H), 2.70 (s, 3H). ^{13}C NMR (DMSO-d_6): δ 172.78, 163.44, 150.16, 143.39, 138.83, 138.60, 134.38, 133.50, 130.81, 126.90, 126.01, 124.53, 123.56, 122.78, 120.38, 111.95, 106.34, 19.86. HRMS (ESI, m/z): calculated for $C_{18}H_{16}N_3O_5S$ $[M+H]^+$ 386.0805; found 386.0810.

4.1.1.11. (E)-2-hydroxy-3-((4-methyl-3-sulfamoylphenyl)diazenyl)-1-naphthoic acid (9k). The product was obtained as red solid using method B. Yield (81%). ^{1}H NMR (400 MHz, DMSO-d_6): δ 15.51 (s, 1H), 8.58 (d, J = 8.4 Hz, 1H), 8.35 (s, 1H), 8.00 (d, J = 9.2 Hz, 2H), 7.83 (d, J = 7.6 Hz, 1H), 7.67 -7.47 (m, 6H), 6.99 (d, J = 9.2 Hz, 1H), 2.65 (s, 3H). ^{13}C NMR (DMSO-d_6): δ 167.05, 143.72, 143.59, 139.82, 135.71, 133.67, 132.53, 129.33, 129.07, 128.90, 127.94, 125.89, 123.34, 122.53, 121.26, 117.08, 19.62. HRMS (ESI, m/z): calculated for $C_{18}H_{16}N_3O_5S$ $[M+H]^+$ 386.0805; found 386.0833.

4.1.1.12. (E)-3-((4-amino-6-hydroxynaphthalen-1-yl)diazenyl)benzenesulfonamide (9l). The product was obtained as dark purple solid using method A. Yield (79%). ^{1}H NMR (400 MHz, DMSO-d_6): δ 8.66 (d, J = 8.8 Hz, 1H), 8.31 (m, 1H), 8.19 (s, 1H), 8.00 (d, J = 6.4 Hz, 1H), 7.70-7.66 (m, 2H), 7.60-7.54

(m, NMR (DMSO-d_6): δ 156.90, 146.30, 145.48, 134.19, 130.25, 128.05, 125.30, 123.24, 122.73, 121.36, 118.16, 117.34, 116.10, 114.27, 107.74, 107.40. HRMS (ESI, m/z): calculated for $C_{16}H_{15}N_4O_3S$ $[M+H]^+$ 343.0859; found 343.0896.

4.1.1.13. (E)-3-((4-aminonaphthalen-1-yl)diazenyl)benzenesulfonamide (9m). The product was obtained as black solid using method B. Yield (30%). ^{1}H NMR (400 MHz, DMSO-d_6): δ 8.82 (d, J = 8.4 Hz, 1H), 8.37 (m, 2H), 8.25 (s, 1H), 8.06 (d, J = 7.6 Hz, 1H), 7.82-7.68 (m, 3H), 7.64-7.55 (m, 3H), 7.04 (d, J = 8.8 Hz, 1H). ^{13}C NMR (DMSO-d_6): δ 159.76, 145.98, 145.49, 135.19, 133.20, 132.15, 130.24, 127.14, 125.45, 125.34, 124.48, 123.32, 122.88, 121.51, 115.99, 114.35. HRMS (ESI, m/z): calculated for $C_{16}H_{15}N_4O_2S$ $[M+H]^+$ 327.0910; found 327.0904.

4.1.1.14. (E)-3-((2-hydroxynaphthalen-1-yl)diazenyl)benzenesulfonamide (9n). The product was obtained as orange solid using method B. Yield (40%). ^{1}H NMR (400 MHz, DMSO-d_6): δ 8.53 (d, J = 8.4 Hz, 1H), 8.28 (s, 1H), 8.03-7.97 (m, 2H), 7.80-7.69 (m, 3H), 7.64 (t, J = 7.6 Hz, 1H), 7.58 (s, 2H), 7.49 (t, J = 7.6 Hz, 1H), 6.90 (d, J = 9.2 Hz, 1H). ^{13}C NMR (DMSO-d_6): δ 171.77, 145.85, 145.08, 141.43, 132.77, 130.83, 129.95, 129.58, 129.29, 128.20, 126.67, 124.58, 124.14, 122.28, 121.67, 114.86. HRMS (ESI, m/z): calculated for $C_{16}H_{14}N_3O_3S$ $[M+H]^+$ 328.0750; found 328.0757.

4.1.1.15. (E)-3-((7-hydroxy-2-oxo-2H-chromen-6-yl)diazenyl)benzenesulfonamide (9o). The product was obtained as brown solid using method B. Yield (83%). ^{1}H NMR (400 MHz, DMSO-d_6): δ 11.67 (s, 1H), 8.36 (s, 1H), 8.22 (d, J = 8.0 Hz, 1H), 8.12-8.06 (m, 2H), 7.99 (d, J = 7.6 Hz, 1H), 7.81 (t, J = 8.0 Hz, 1H), 7.55 (s, 2H), 7.03 (s, 1H), 6.36 (d, J = 9.6 Hz, 1H). ^{13}C NMR (DMSO-d_6): δ 159.61, 158.90, 157.40, 151.63, 145.49, 144.65, 136.63, 130.39, 127.96, 126.78, 119.72, 118.74, 113.39, 111.97, 104.54. HRMS (ESI, m/z): calculated for $C_{15}H_{12}N_3O_5S$ $[M+H]^+$ 346.0492; found 346.0506.

4.1.1.16. (E)-2-hydroxy-5-((3-sulfamoylphenyl)diazenyl)benzoic acid (9p). The product was obtained as yellow solid using method B. Yield (39%). ^{1}H NMR (400 MHz, DMSO-d_6): δ 8.39 (s, 1H), 8.26 (s, 1H), 8.14-8.11 (m, 2H), 7.97 (d, J = 7.2 Hz, 1H), 7.80 (t, J = 7.2 Hz, 1H), 7.54 (s, 2H), 7.19 (d, J = 8.8 Hz, 1H). ^{13}C NMR (DMSO-d_6): δ 171.24, 164.01, 151.76, 145.48, 144.39, 130.41, 129.08, 127.66, 126.78, 126.30, 118.58, 118.07, 113.86. HRMS (ESI, m/z): calculated for $C_{13}H_{12}N_3O_5S$ $[M+H]^+$ 322.0492; found 322.0496.

4.1.1.17. (E)-1-hydroxy-4-((3-sulfamoylphenyl)diazenyl)-2-naphthoic acid (9q)

The product was obtained as dark red solid using method B. Yield (80%). ^{1}H NMR (400 MHz, DMSO-d_6): δ 12.89 (s, 1H), 8.84 (d, J = 8.8 Hz, 1H), 8.35 (d, J = 8.4 Hz, 1H), 8.23 (s, 1H), 8.10-8.0 (m, 5H), 7.85 (t, J = 7.6 Hz, 1H), 7.70 (t, J = 7.6 Hz, 1H), 7.30 (m, 1H), 6.88 (m, 1H). ^{13}C NMR (DMSO-d_6): δ 172.52, 169.08, 164.53, 153.74, 143.43, 138.40, 134.56, 130.92, 127.20, 126.91, 124.63, 123.62, 122.80, 112.70, 108.57, 106.85. HRMS (ESI, m/z): calculated for $C_{17}H_{14}N_3O_5S$ $[M+H]^+$ 372.0649; found 372.0261.

4.1.1.18. (E)-3-((8-hydroxyquinolin-5-yl)diazenyl)benzenesulfonamide (9r). The product was obtained as brown solid using method B. Yield (76%). ^{1}H NMR (400 MHz, DMSO-d_6): δ 9.76 (d, J = 7.6 Hz, 1H), 9.16 (m, 1H), 8.40 (s, 1H), 8.22-8.12 (m, 3H), 7.99 (m, 1H), 7.81 (m, 1H), 7.64-7.56 (m, 3H). ^{13}C NMR (DMSO-d_6): δ 155.17, 151.96, 146.31, 145.59, 139.17, 137.68, 131.50, 130.41, 128.29, 127.65, 126.23, 123.84, 118.81, 117.30, 114.98. HRMS (ESI, m/z): calculated for $C_{15}H_{13}N_4O_3S$ $[M+H]^+$ 329.0703; found 329.0708.

4.1.1.19. (E)-3-((4-hydroxynaphthalen-1-yl)diazenyl)benzenesulfonamide (9s). The product was obtained as orange solid using method B. Yield (33%). ^{1}H NMR (400 MHz, DMSO-d_6): δ 8.79 (s, 1H), 8.25- 8.18 (m, 2H), 8.03 (s, 2H), 7.81-7.73 (m, 3H), 7.62-7.56 (m, 3H), 6.95 (m, 1H). ^{13}C NMR (DMSO-d_6): δ. 158.58, 152.64, 145.46, 139.44, 132.81, 130.33, 128.12, 126.90, 126.68, 125.65, 124.38, 122.51, 118.04, 114.63, 108.57. HRMS (ESI, m/z): calculated for $C_{16}H_{14}N_3O_3S$ $[M+H]^+$ 328.0750; found 328.0744.

4.1.1.20. (E)-3-((4-hydroxyphenyl)diazenyl)benzenesulfonamide (9t). The product was obtained as yellowish brown solid using method B. Yield (22%). ^{1}H NMR (400 MHz, DMSO-d_6): δ 10.46 (s, 1H), 8.21 (s, 1H), 8.05 (d, J = 7.7 Hz, 1H), 7.93 (d, J = 7.5 Hz, 1H), 7.86 (d, J = 8.6 Hz, 2H), 7.77 (t, J = 7.8 Hz, 1H), 7.52 (s, 2H), 6.97 (d, J = 8.6 Hz, 2H). ^{13}C NMR (DMSO-d_6): δ 161.64, 152.02, 145.38, 145.13, 130.29, 127.04, 126.56, 125.28, 117.73, 116.13. HRMS (ESI, m/z): calculated for $C_{12}H_{12}N_3O_3S$ $[M+H]^+$ 278.0594; found 278.0545.

4.1.1.21. (E)-5-(phenyldiazenyl)quinolin-8-ol (9u). The product was obtained as purple solid using method B. Yield (50%). ^{1}H NMR (400 MHz, DMSO-d_6): δ 9.31 (d, J = 8.4 Hz, 1H), 8.99 (s, 1H), 8.0-7.98 (m, 3H), 7.78-7.75 (m, 1H), 7.63-7.54 (m, 3H), 7.24 (d, J = 8.4 Hz, 1H). ^{13}C NMR (DMSO-d_6): δ 157.62, 152.56, 149.01, 138.63, 137.94, 131.81, 130.77, 129.41, 127.52, 123.20, 122.48, 114.80, 111.66. HRMS (ESI, m/z): calculated for $C_{15}H_{12}N_3O$ $[M+H]^+$ 250.0975; found 250.0983.

4.1.1.22. (E)-3-((8-hydroxyquinolin-5-yl)diazenyl)benzoic acid (9v). The product was obtained as orange solid using method B. Yield (70%). ^{1}H NMR (400 MHz, DMSO-d_6): δ 9.29 (d, J = 8.0 Hz, 1H), 9.00 (s, 1H), 8.44 (s, 1H), 8.22 (d, J = 6.8 Hz, 1H), 8.10-8.03 (m, 2H), 7.81-7.71 (m, 2H), 7.25 (d, J = 8.4 Hz, 1H). ^{13}C NMR (DMSO-d_6): δ 166.85, 158.06, 152.54, 149.09, 138.61, 137.93, 132.19, 131.71, 131.11, 129.85, 127.57, 126.48, 123.41, 122.96, 115.47, 111.74. HRMS (ESI, m/z): calculated for $C_{16}H_{12}N_3O_3$ $[M+H]^+$ 294.0873; found 294.0880.

4.1.1.23. (E)-4-((8-hydroxyquinolin-5-yl)diazenyl)benzoic acid (9w). The product was obtained as brown solid using method B. Yield (100%). ^{1}H NMR (400 MHz, DMSO-d_6): δ 9.65 (d, J = 8.8 Hz, 1H), 9.09 (s, 1H), 8.17-8.2 (m, 6H), 7.42 (d, J = 8.8 Hz, 1H).^{13}C NMR (DMSO-d_6): δ. 166.99, 154.35, 147.20, 137.92, 137.58, 133.65, 132.15, 130.86, 128.70, 124.15, 122.38, 117.41, 115.02. HRMS (ESI, m/z): calculated for $C_{16}H_{12}N_3O_3$ $[M+H]^+$ 294.0873; found 294.0872.

4.1. ***yl)diazenyl)benzenesulfonic acid (9x)***. The product was obtained as dark red solid using method B. Yield (75%). ^{1}H NMR (400 MHz, DMSO-d_6): δ 9.66 (d, J = 6.4 Hz, 1H), 9.10 (s, 1H), 8.12 (d, J = 7.6 Hz, 1H), 7.99 (m, 3H), 7.82 (m, 2H), 7.40 (d, J = 7.6 Hz, 1H). HRMS (ESI, m/z): calculated for $C_{15}H_{12}N_3O_4S$ $[M+H]^+$ 330.0543; found 330.0554.

4.2. In vitro enzyme inhibition assay

The Glo-I inhibitory activity of the synthesized compounds was performed *in vitro* using the recombinant human Glo-I (R&D Systems® Corporation, USA) as detailed elsewhere.[29, 39] Using a double-beam UV–Vis spectrophotometer (Biotech engineering management Co. Ltd., UK), the percent of Glo-I inhibition for each tested compound was measured through three independent experiments performed in triplicate, and the average was calculated. Calculation of the IC_{50} values of all compounds was performed using GraphPad Prism 6 (2012).

4.3. In silico design

4.3.1. Compounds preparation

All synthesized compounds were sketched using ChemBioDraw Ultra 12, imported into discovery studio (DS) and converted into their corresponding 3D structures using "prepare ligand" protocol. This protocol was utilized to perform many tasks involving the assignment of proper bond orders, generation of ionization states, as well as assignment of chemical isomers and tautomers. Default parameters were utilized except for the pH-based ionization, which was changed into 7.2-7.6 range.

4.3.2 Protein preparation

The crystal structure of Glo-I in complex with N-hydroxypyridone derivative inhibitor (HPU) was retrieved from the Protein Data Bank (PDB code 3W0T: resolution 1.35 Å) to serve as docking template.[40-41] The structural model was checked for missing loops, alternate conformations, or incomplete residues using Protein Report tool within DS. The Prepare Protein protocol within DS was applied to clean the crystal structure, correct connectivity and bond order, standardize atom names, and protonate protein at pH of 7.4.[42-43]

4.3.3 Molecular Docking

Prior to molecular docking, the prepared crystal structure was solvated and energy-minimized, using the Simulation Tools within DS. Following minimization, water molecules were deleted and the co-crystalized ligand (HPU) was used to define the binding site using the Define and Edit Binding Site tool, then it was deleted. The radius of the generated sphere was chosen to be 10 Å radius. Subsequently, the Dock ligands (CDOCKER) protocol was employed using default parameters.[44]

4.3.4 ADMET descriptors and Toxicity parameters

The ADMET descriptors were calculated using the ADMET Descriptors protocol in DS. For toxicity parameters, the *Toxicity Prediction (TOPKAT)* protocol in DS.

Acknowledgments

rom Deanship of Research at the Jordan University of Science and Technology (Grant No. 513/2019). The high-resolution mass spectrometry data were acquired in the College of Arts and Sciences and Mathematics Instrumentation Center at the University of Toledo, 2801 W Bancroft drive, Toledo, OH, USA.

References and notes

1. Siegel, R.; Ma, J.; Zou, Z.; Jemal, A., Cancer statistics, 2014. *CA: a cancer journal for clinicians* **2014,** *64* (1), 9-29.
2. Prendergast, G. C.; Jaffee, E. M., Cancer immunologists and cancer biologists: why we didn't talk then but need to now. *Cancer Research* **2007,** *67* (8), 3500-3504.
3. Vince, R.; Wadd, W. B., Glyoxalase inhibitors as potential anticancer agents. *Biochemical and biophysical research communications* **1969,** *35* (5), 593-598.
4. Vince, R.; Daluge, S., Glyoxalase inhibitors. A possible approach to anticancer agents. *Journal of medicinal chemistry* **1971,** *14* (1), 35-37.
5. Racker, E., The mechanism of action of glyoxalase. *Journal of Biological Chemistry* **1951,** *190* (2), 685-696.
6. Chasseaud, L., Functions of glutathione: Biochemical, physiological, toxicological and clinical aspects: edited by A. Larsson, S. Orrenius, A, Holmgren and B. Munnervik, Raven Press, 1983.(xix+ 403 pages) ISBN 0 89 004908 4. Elsevier Current Trends: 1985.
7. Carrington, S., The glyoxalase enigma. The biological consequences of a ubiquitous enzyme. *IRCS Med Sci* **1986,** *14*, 763-768.
8. Richard, J. P., Kinetic parameters for the elimination reaction catalyzed by triosephosphate isomerase and an estimation of the reaction's physiological significance. *Biochemistry* **1991,** *30* (18), 4581-4585.
9. Degenhardt, T. P.; Thorpe, S. R.; Baynes, J. W., Chemical modification of proteins by methylglyoxal. *Cellular and molecular biology (Noisy-le-Grand, France)* **1998,** *44* (7), 1139-45.
10. Ramasamy, R.; Vannucci, S. J.; Yan, S. S. D.; Herold, K.; Yan, S. F.; Schmidt, A. M., Advanced glycation end products and RAGE: a common thread in aging, diabetes, neurodegeneration, and inflammation. *Glycobiology* **2005,** *15* (7), 16R-28R.
11. Ahmed, M. U.; FRYE, E. B.; Degenhardt, T. P.; Thorpe, S. R.; Baynes, J. W., Nε-(carboxyethyl) lysine, a product of the chemical modification of proteins by methylglyoxal, increases with age in human lens proteins. *Biochemical Journal* **1997,** *324* (2), 565-570.
12. Nakaya, K.; Takenaka, O.; Horinishi, H.; Shibata, K., Reactions of glyoxal with nucleic acids, nucleotides and their component bases. *Biochimica et Biophysica Acta (BBA)-Nucleic Acids and Protein Synthesis* **1968,** *161* (1), 23-31.
13. Thornalley, P. J., The glyoxalase system: new developments towards functional characterization of a metabolic pathway fundamental to biological life. *Biochemical Journal* **1990,** *269* (1), 1.
14. Sousa Silva, M.; Gomes, Ricardo A.; Ferreira, Antonio E. N.; Ponces Freire, A.; Cordeiro, C., The glyoxalase pathway: the first hundred years… and beyond. *Biochemical Journal* **2013,** *453* (1), 1-15.
15. Thornalley, P. J., Glutathione-dependent detoxification of α-oxoaldehydes by the glyoxalase system: involvement in disease mechanisms and antiproliferative activity of glyoxalase I inhibitors. *Chemico-biological interactions* **1998,** *111*, 137-151.
16. Rulli, A.; Carli, L.; Romani, R.; Baroni, T.; Giovannini, E.; Rosi, G.; Talesa, V., Expression of glyoxalase I and II in normal and breast cancer tissues. *Breast cancer research and treatment* **2001,** *66* (1), 67-72.
17. Antognelli, C.; Baldracchini, F.; Talesa, V. N.; Costantini, E.; Zucchi, A.; Mearini, E., Overexpression of glyoxalase system enzymes in human kidney tumor. *The Cancer Journal* **2006,** *12* (3), 222-228.
18. Mearini, E.; Romani, R.; Mearini, L.; Antognelli, C.; Zucchi, A.; Baroni, T.; Porena, M.; Talesa, V., Differing expression of enzymes of the glyoxalase system in superficial and invasive bladder carcinomas. *European Journal of Cancer* **2002,** *38* (14), 1946-1950.
19. Sakamoto, H.; Mashima, T.; Kizaki, A.; Dan, S.; Hashimoto, Y.; Naito, M.; Tsuruo, T., Glyoxalase I is involved in resistance of human leukemia cells to antitumor agent-induced apoptosis. *Blood* **2000,** *95* (10), 3214-8.
20. Lo, T. W.; Thornalley, P. J., Inhibition of proliferation of human leukaemia 60 cells by diethyl esters of glyoxalase inhibitors in vitro. *Biochemical pharmacology* **1992,** *44* (12), 2357-63.
21. Thornalley, P., Glyoxalase I–structure, function and a critical role in the enzymatic defence against glycation. *Biochemical Society Transactions* **2003,** *31* (6), 1343-1348.
22. Al-Balas, Q.; Hassan, M.; Al-Oudat, B.; Alzoubi, H.; Mhaidat, N.; Almaaytah, A., Generation of the first structure-based pharmacophore model containing a selective "zinc binding group" feature to identify potential glyoxalase-1 inhibitors. *Molecules* **2012,** *17* (12), 13740-58.
23. Al-Balas, Q. A.; Hassan, M. A.; Al-Shar'i, N. A.; Al Jabal, G. A.; Almaaytah, A. M., Recent Advances in Glyoxalase-I Inhibition. *Mini reviews in medicinal chemistry* **2019,** *19* (4), 281-291.
24. Vince, R.; Daluge, S.; Wadd, W. B., Inhibition of glyoxalase I by S-substituted glutathiones. *Journal of medicinal chemistry* **1971,** *14* (5), 402-404.
25. Hamilton, D.; Creighton, D., Inhibition of glyoxalase I by the enediol mimic S-(N-hydroxy-N-methylcarbamoyl) glutathione. The possible basis of a tumor-selective anticancer strategy. *Journal of Biological Chemistry* **1992,** *267* (35), 24933-24936.
26. Murthy, N. S.; Bakeris, T.; Kavarana, M. J.; Hamilton, D. S.; Lan, Y.; Creighton, D. J., S-(N-aryl-N-hydroxycarbamoyl) glutathione derivatives are tight-binding inhibitors of glyoxalase I and slow substrates for glyoxalase II. *Journal of medicinal chemistry* **1994,** *37* (14), 2161-2166.
27. Liu, M.; Yuan, M.; Luo, M.; Bu, X.; Luo, H.-B.; Hu, X., Binding of curcumin with glyoxalase I: Molecular docking, molecular dynamics simulations, and kinetics analysis. *Biophysical chemistry* **2010,** *147* (1-2), 28-34.
28. Yuan, M.; Luo, M.; Song, Y.; Xu, Q.; Wang, X.; Cao, Y.; Bu, X.; Ren, Y.; Hu, X., Identification of curcumin derivatives as human glyoxalase I inhibitors: A combination of biological evaluation, molecular docking, 3D-QSAR and molecular dynamics simulation studies. *Bioorganic & medicinal chemistry* **2011,** *19* (3), 1189-1196.
29. Al-Balas, Q. A.; Hassan, M. A.; Al-Shar'i, N. A.; Mhaidat, N. M.; Almaaytah, A. M.; Al-Mahasneh, F. M.; Isawi, I. H., novel glyoxalase-i inhibitors possessing a "zinc-binding feature" as potential anticancer agents. *Drug design, development and therapy* **2016,** *10*, 2623.
30. Zhang, H.; Zhai, J.; Zhang, L.; Li, C.; Zhao, Y.; Chen, Y.; Li, Q.; Peng Hu, X., In Vitro Inhibition of Glyoxalase Ц# 134; by Flavonoids: New Insights from Crystallographic Analysis. *Current topics in medicinal chemistry* **2016,** *16* (4), 460-466.
31. Yadav, A.; Kumar, R.; Sunkaria, A.; Singhal, N.; Kumar, M.; Sandhir, R., Evaluation of potential flavonoid inhibitors of glyoxalase-I based on virtual screening and in vitro studies. *Journal of Biomolecular Structure and Dynamics* **2016,** *34* (5), 993-1007.
32. Chiba, T.; Ohwada, J.; Sakamoto, H.; Kobayashi, T.; Fukami, T. A.; Irie, M.; Miura, T.; Ohara, K.; Koyano, H., Design and evaluation of azaindole-substituted N-hydroxypyridones as glyoxalase I inhibitors. *Bioorganic & medicinal chemistry letters* **2012,** *22* (24), 7486-7489.
33. Takasawa, R.; Tao, A.; Saeki, K.; Shionozaki, N.; Tanaka, R.; Uchiro, H.; Takahashi, S.; Yoshimori, A.; Tanuma, S.-i., Discovery of a new type inhibitor of human glyoxalase I by

myr... Al-
chemistry letters **2011,** *21* (14), 4337-4342.
34. More, S. S.; Vince, R., Design, synthesis, and binding studies of bidentate Zn-chelating peptidic inhibitors of glyoxalase-I. *Bioorganic & medicinal chemistry letters* **2007,** *17* (13), 3793-3797.
35. Perez, C.; Barkley-Levenson, A. M.; Dick, B. L.; Glatt, P. F.; Martinez, Y.; Siegel, D.; Momper, J. D.; Palmer, A. A.; Cohen, S. M., Metal-Binding Pharmacophore Library Yields the Discovery of a Glyoxalase 1 Inhibitor. *Journal of Medicinal Chemistry* **2019,** *62* (3), 1609-1625.
36. Al-Sha'er, M. A.; Al-Balas, Q. A.; Hassan, M. A.; Al Jabal, G. A.; Almaaytah, A. M., Combination of pharmacophore modeling and 3D-QSAR analysis of potential glyoxalase-I inhibitors as anticancer agents. *Computational Biology and Chemistry* **2019,** *80*, 102-110.
37. Carta, F.; Maresca, A.; Scozzafava, A.; Vullo, D.; Supuran, C. T., Carbonic anhydrase inhibitors. Diazenylbenzenesulfonamides are potent and selective inhibitors of the tumor-associated isozymes IX and XII over the cytosolic isoforms I and II. *Bioorg Med Chem* **2009,** *17* (20), 7093-9.
38. Al-Shar'i, N. A.; Al-Rousan, E. K.; Fakhouri, L. I.; Al-Balas, Q. A.; Hassan, M. A., Discovery of a nanomolar glyoxalase-I inhibitor using integrated ligand-based pharmacophore modeling and molecular docking. *Medicinal Chemistry Research* **2019,** *29* (3), 356-376.
Shar, N.; M Almaaytanb, A.; El-Elimata, T., Novel thiazole carboxylic acid derivatives possessing a "zinc binding feature" as potential human glyoxalase-i inhibitors. *Letters in Drug Design & Discovery* **2017,** *14* (11), 1324-1334.
40. Berman, H. M., The Protein Data Bank: a historical perspective. *Acta crystallographica. Section A, Foundations of crystallography* **2008,** *64* (Pt 1), 88-95.
41. Berman, H. M.; Battistuz, T.; Bhat, T. N.; Bluhm, W. F.; Bourne, P. E.; Burkhardt, K.; Feng, Z.; Gilliland, G. L.; Iype, L.; Jain, S.; Fagan, P.; Marvin, J.; Padilla, D.; Ravichandran, V.; Schneider, B.; Thanki, N.; Weissig, H.; Westbrook, J. D.; Zardecki, C., The Protein Data Bank. *Acta crystallographica. Section D, Biological crystallography* **2002,** *58* (Pt 6 No 1), 899-907.
42. Spassov, V. Z.; Flook, P. K.; Yan, L., LOOPER: a molecular mechanics-based algorithm for protein loop prediction. *Protein engineering, design & selection : PEDS* **2008,** *21* (2), 91-100.
43. Spassov, V. Z.; Yan, L., A fast and accurate computational approach to protein ionization. *Protein Sci* **2008,** *17* (11), 1955-1970.
44. Wu, G.; Robertson, D. H.; Brooks, C. L., 3rd; Vieth, M., Detailed analysis of grid-based molecular docking: A case study of CDOCKER-A CHARMm-based MD docking algorithm. *Journal of computational chemistry* **2003,** *24* (13), 1549-62.

Declaration of interests

☒ The authors declare that they have no known competing financial interests or personal relationships that could have appeared to influence the work reported in this paper.

☐The authors declare the following financial interests/personal relationships which may be considered as potential competing interests: